

## Three-body breakup in dissociative electron attachment to the water molecule

Daniel J. Haxton,<sup>1,\*</sup> Thomas N. Rescigno,<sup>2,†</sup> and C. William McCurdy<sup>2,3,‡</sup>

<sup>1</sup>*Department of Physics and JILA, University of Colorado, Boulder, Colorado 80309, USA*

<sup>2</sup>*Chemical Sciences, Lawrence Berkeley National Laboratory, Berkeley, California 94720, USA*

<sup>3</sup>*Department of Applied Science and Department of Chemistry, University of California, Davis, California 95616, USA*

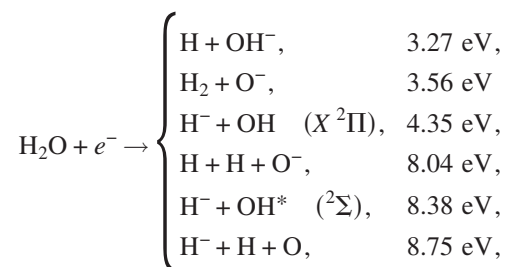
(Received 17 July 2008; published 8 October 2008)

We report the results of *ab initio* calculations on dissociative electron attachment to water that demonstrate the importance of including three-body breakup in the dissociation dynamics. While three-body breakup is ubiquitous in the analogous process of dissociative recombination, its importance in low-energy dissociative electron attachment to a polyatomic target has not previously been quantified. Our calculations indicate that three-body breakup is a major component of the observed  $O^-$  cross section. Our studies suggest that the local complex potential model provides a generally accurate picture of the experimentally observed features in this polyatomic system.

DOI: [10.1103/PhysRevA.78.040702](https://doi.org/10.1103/PhysRevA.78.040702)

PACS number(s): 34.80.Ht, 03.65.Nk

Dissociative electron attachment (DEA) to the water molecule,



is a resonant process that involves the capture of a free electron into a transient negative ion state that subsequently dissociates to produce neutral and ionic fragments. Previous experimental [1–10] and theoretical studies [11–19] have characterized the various breakup channels and the three metastable anion states involved in the DEA process—the  $^2B_1$ ,  $^2A_1$ , and  $^2B_2$  electronic Feshbach resonances with peaks near 6.4, 8.4, and 12 eV, respectively. DEA in water is governed by complex electronic and nuclear dynamics involving, as we have previously shown [16], anion surfaces that interact via conical intersection and Renner-Teller effects. Our previous studies on this system [14–19], involving anion surfaces computed *ab initio* and nuclear dynamics calculations carried out in full dimensionality within the local complex potential model, succeeded in giving a quantitatively accurate description of the major DEA channel— $H^- + OH$  production through the  $^2B_1$  state—as well as a qualitatively accurate description of many features associated with the minor channels, with two notable exceptions. Our calculations significantly underestimated the cross section for  $O^-$  production via the  $^2B_2$  state and produced a zero result for  $O^-$  production via the  $^2A_1$  state, although the latter process has been clearly observed experimentally. The purpose of this Rapid

Communication is to resolve these two discrepancies between theory and experiment.

Our work to date has considered the breakup of transient  $H_2O^-$  species only into diatomic fragments,  $H^- + OH$  and  $O^- + H_2$ , and did not treat three-body breakup. Three-body DEA has yet to be studied theoretically, for any system. While three-body breakup is known to be important in dissociative recombination of polyatomic ions, where three-body channels are generally open even at threshold, for DEA the process has yet to be quantified. The three-body channels  $H^- + H + O$  and  $O^- + H + H$  open up within the second ( $^2A_1$ ) DEA peak, but are energetically closed for the lowest  $^2B_1$  resonance. In an experiment on DEA to  $D_2O$ , Curtis and Walker [9] observed the opening of the lower three-body channel, as discerned through the kinetic energy distribution of the  $O^-$  fragment. However, because of the large O atom to  $H_2$  mass ratio, such a measurement is difficult, and a quantitative experimental determination of the final-state branching ratios among the two- and three-body breakup channels has yet to be published.

There is strong reason to believe that three-body breakup is important for describing DEA leading to  $O^-$  production. In particular, examination of the shape of the  $^2A_1$  surface suggests that three-body breakup may be the key to describing  $O^-$  production via this resonance. The  $^2A_1$  ( $1^2A'$ ) electronic surface slopes downward toward linear H-O-H geometry and is dissociative along the OH bonds. It provides a path for symmetric dissociation of the OH bonds to produce  $O^- + H + H$ , but also slopes downward toward the  $H^- + OH$  asymptotes. Similarly, the  $^2B_2$  diabatic surface, which equals the  $^2B_2$  adiabatic surface for  $C_{2v}$  geometries, provides a path toward symmetric dissociation through the conical intersection with the  $^2A_1$  state. Symmetric dissociation of the  $^2B_2$  state from the equilibrium geometry of the neutral leads to the  $O^- + H + H$  three-body asymptote.

Our methodology is very similar to that used in our previous calculations, so we provide only a brief summary here. We use the local complex potential or “boomerang” model [20–24] in which the nuclear motion is determined by a driven Schrödinger equation that describes the dynamics of the metastable  $H_2O^-$  electronic state(s) that correlate(s) with the neutral+anion fragments:

\*dhaxton@jila.colodado.edu

†tnrescigno@lbl.gov

‡cwmccurdy@lbl.gov

$$(E - H)\xi_{\nu_i}(\vec{q}) = \phi_{\nu_i}(\vec{q}, 0), \quad (1)$$

where the Born-Oppenheimer anion Hamiltonian is

$$H = K_{\vec{q}} + E_R(\vec{q}) - \frac{i\Gamma(\vec{q})}{2}, \quad (2)$$

the nuclear degrees of freedom are collectively denoted by  $\vec{q}$ , and the nuclear kinetic energy is denoted by  $K_{\vec{q}}$ .  $E_R$  is the location of the resonance and  $\Gamma$  is its width as functions of nuclear geometry. The energy  $E$  is the energy of the entire system, namely, that of the target molecular state plus the kinetic energy of the incident electron. The driving term  $\phi_{\nu_i}$  is defined as

$$\phi_{\nu_i}(\vec{q}, 0) = \sqrt{\frac{\Gamma_0(\vec{q})}{2\pi}} \chi_{\nu_i}(\vec{q}), \quad (3)$$

where  $\chi_{\nu_i}$  is the initial vibrational wave function of the neutral target molecule, whose quantum numbers are collectively denoted by  $\nu_i$ , and  $\Gamma_0$  is the partial width with respect to decay to the ground electronic state.

We have used our previously calculated [18] complex-valued potential energy surfaces for the three metastable electronic states. As in our previous calculations of the two-body cross sections [19], we used the diabaticized  ${}^2A_1$  and  ${}^2B_2$  surfaces that account for the conical intersection between these states. The nuclear wave equation, Eq. (1), can be solved using time-dependent methods by representing the nuclear Green's function  $(E - H + i\epsilon)^{-1}$  as the Fourier transform of the corresponding propagator [25]. The time-dependent nuclear dynamics were calculated using the multiconfiguration time-dependent Hartree algorithm [26–28] and the numerical implementation by Worth *et al.* [29].

In our previous calculations on two-body breakup, we employed Jacobi coordinate systems  $(R, r, \gamma)$  based upon the diatomic fragment to be analyzed. Such a coordinate system is inappropriate for three-body breakup, as the asymptotic region is not well defined in terms of a single degree of freedom. Instead, we use hyperspherical coordinates. Hyperspherical coordinates have been applied fruitfully to the problem of dissociative recombination, for example, to that of  $H_3^+$  in Ref. [30]; such calculations have yielded the branching ratio into two-body versus three-body breakup. We use Delves-type [31,32] hyperspherical coordinates, in which there is only one dissociative degree of freedom, the hyperradius  $\mathbf{R}$ . These coordinates are based upon the Jacobi coordinate system in which  $r$  is an OH bond length, and include the Jacobi angle  $\gamma$ , a hyperangle  $\theta$ , and the hyperradius  $\mathbf{R}$ :

$$\mathbf{R} = \sqrt{R^2 + \frac{\mu_r}{\mu_R} r^2}, \quad \theta = \tan^{-1} \sqrt{\frac{\mu_r}{\mu_R} \frac{R}{r}}, \quad (4)$$

where the reduced masses correspond to the Jacobi coordinates. Further details of our numerical implementation will be forthcoming in a future presentation [33].

In order to calculate a three-body breakup cross section, our strategy is to calculate, in hyperspherical coordinates, the total DEA cross section and then subtract the two-body cross sections from the total cross section. As in our earlier studies

[15,19], the two-body cross sections were obtained from the outgoing flux projected onto the bound rovibrational states of OH or  $H_2$ . For the present study, we have fully converged the  $H^- + OH$  Jacobi coordinate calculations for DEA via the  ${}^2B_2$  state and may now better resolve the branching ratio between  $H^- + OH$  ( ${}^2\Sigma$ ) and  $H^- + OH$  ( $X {}^2\Pi$ ). The  ${}^2A_1$  calculation for this coordinate system was also redone. The  $O^- + H_2$  results are unchanged.

The three-body breakup threshold is 8.04 eV for  $H + H + O^-$ , and 8.75 eV for  $H^- + H + O$ ; the onsets for the experimental peaks for  $O^-$  and  $H^-$  via  ${}^2A_1$  are approximately 7.9 and 7.5 eV [10]. Our potential energy surfaces, however, do not distinguish between the three-body asymptotes. As described in a previous publication [16], the full set of curves affecting the dynamics on the three resonant curves numbers at least five; there are eleven distinct seams of intersection among these. Our surfaces do not describe every one of these features. On the  ${}^2A_1$  ( $1 {}^2A'$ ) surface, the  $OH + H^-$  and  $H + OH^-$  curves intersect as a function of OH distance, which will lead to coupling between these channels for high OH or  $OH^-$  vibrational levels. As the interacting curves are nearly parallel, we do not expect this feature of the physical surfaces to affect the branching ratio between three- and two-body breakup, except near onset. We have patched our calculated surface so that its asymptote lies exactly between the two physical asymptotes. As our studies of the two-body channels in DEA via the  ${}^2A_1$  state yielded zero  $O^- + H_2$  cross section, we make the hypothesis that the  $O^-$  observed for DEA via the  ${}^2A_1$  resonance is entirely due to three-body dissociation.

While we expect the approximation to the  ${}^2A_1$  surface to have little influence on our results for three-body breakup, the true  ${}^2B_2$  surface has a feature that we have not included in the calculated surface, which may affect the dynamics significantly. As explained in Ref. [16], this feature is unique to metastable states, not being possible for bound states. It is a branch-point degeneracy seam with another metastable  ${}^2B_2$  state that leads to a double-valuedness of the surface; a transit about the seam exchanges the states. This seam is analogous to either member of the double seams in Refs. [34,35]. The two three-body asymptotes of this surface are  $O^- + H + H$  and  $O({}^2D) + H^- + H$ . The seam intersects the  $C_{2v}$  plane at a moderately stretched and squeezed geometry [16]. Because the gradient of the  ${}^2B_2$  surface will force the system toward this geometry, it is likely that the double-valuedness of the surface, and our approximation to it, will affect the dynamics. However, it is unclear how the approximation would affect three-body breakup. There is no experimental evidence for production of  $O({}^2D)$ ; however, the upper component of the double-valued set has a short lifetime and therefore it is likely that any  $O({}^2D)$  produced is not accompanied by an  $H^-$  anion and is therefore invisible in the experiments performed to date. We truncate the  ${}^2B_2$  surface to its lower three-body asymptote,  $O^- + H + H$ .

In Fig. 1 we plot the results for DEA via the  ${}^2A_1$  state. We calculate a significant three-body cross section. We assign our calculated  ${}^2A_1$  three-body breakup cross section to the  $O^-$  channel. This is consistent with the topology of the surfaces, as direct symmetric dissociation of the  ${}^2A_1$  state leads to the  $O^- + H + H$  asymptote. The  $O + H^- + H$  asymptote, on

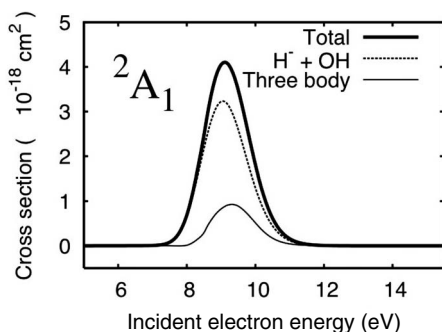


FIG. 1. Two- and three-body cross sections calculated for DEA via the  $^2A_1$  state.

the other hand, is reached near the  $\text{OH}+\text{H}^-$  well, where the surface interacts with the  $\text{OH}^-+\text{H}$  charge exchange state. The two-body cross section is entirely  $\text{H}^-+\text{OH}$ , our calculations yielding zero  $\text{O}^-+\text{H}_2$  production. The subtraction clearly works well, as the onset for three-body breakup is shown to lie above that for two-body breakup.

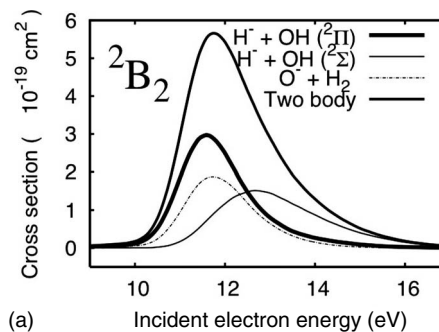
In Fig. 2(a) we plot the results for two-body breakup via the  $^2B_2$  resonance. These results show that, at onset, the cross section is dominated by  $\text{O}^-+\text{H}_2$  and  $\text{H}^-+\text{OH}$  ( $X^2\Pi$ ), the lower-energy channels. The higher  $\text{H}^-+\text{OH}$  ( $^2\Sigma$ ) channel dominates at high energy. Thus, the corresponding branching ratios are energy dependent; the incident electron energy affects the probability of transit through the conical intersection.

We show the kinetic energy release for  $\text{H}^-+\text{OH}$  ( $^2\Sigma$ ,  $^2\Pi$ ) production calculated for DEA via the  $^2B_2$  state in Fig. 2(b). This is a two-dimensional view of the OH peaks in Fig. 2(a). The solid lines indicate the maximum kinetic energy available, given that the diatomic fragment is in its ground rovibrational state. The upper area of contours shows the production of  $\text{H}^-+\text{OH}$  ( $X^2\Pi$ ) from dynamics leading through the conical intersection. The lower area corresponds to  $\text{H}^-+\text{OH}$  ( $^2\Sigma$ ) from dynamics avoiding the conical intersection. We calculate that that the two-body cross sections for both  $\text{OH}$  ( $X^2\Pi$ ) and  $\text{OH}$  ( $^2\Sigma$ ) are dominated by diatoms in low-energy rovibronic states with high kinetic energy release. In this respect we confirm the results of Belic, Landau, and Hall [8], shown in the inset of Fig. 2(b). We note that the  $\text{H}_2$  obtained for this resonance is produced in high rovibrational states, with low kinetic energy release [19].

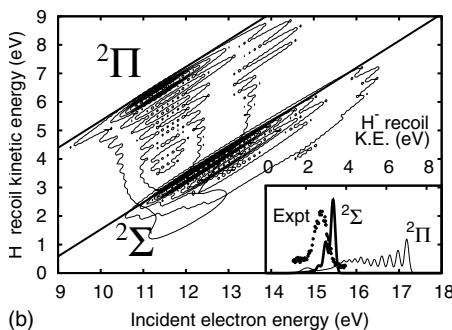
These observations support the conclusion that the  $\text{O}^-+\text{H}+\text{H}$  produced via the  $^2B_2$  resonance is due to the vibrational continuum of  $\text{H}_2+\text{O}^-$  and not that of  $\text{OH}+\text{H}^-$  (interacting with  $\text{OH}^-+\text{H}$ ). Thus, the system does not follow the asymmetric path into one OH well and then outward to three-body breakup; instead,  $\text{O}^-+\text{H}+\text{H}$  is produced along with  $\text{O}^-+\text{H}_2$  in what is probably a more symmetric dissociation path.

In Fig. 2(c) we show the two- and three-body cross sections for DEA via the  $^2B_2$  state. These results indicate that these channels strongly compete, as their cross sections have similar magnitude for all energies.

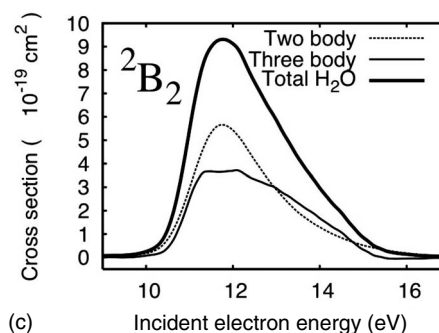
Our final results for  $\text{O}^-$  production in DEA to the water molecule are summarized and compared with the recent results of Fedor *et al.* [10] in Fig. 3. This result replaces that



(a) Incident electron energy (eV)



(b) Incident electron energy (eV)



(c) Incident electron energy (eV)

FIG. 2. Results for DEA via the  $^2B_2$  state, coupled to the  $^2A_1$  state via the conical intersection. (a) Two-body cross sections. (b) Kinetic energy release for DEA leading to  $\text{H}^-+\text{OH}$ . The cross section per unit kinetic energy release is plotted versus incident energy and kinetic energy of  $\text{H}^-+\text{OH}$  separation. The cut at 12 eV is compared with the experimental results of Belic, Landau, and Hall [8] in the inset. (c) Two- and three-body cross sections.

reported in Fig. 3 of Ref. [19]. The  $^2B_1$  result is unchanged from our zero result [19]; not considering  $\text{OH}^-$  production, which is due to nonadiabatic effects and not considered in our studies,  $\text{O}^-$  from the  $^2B_1$  state is the most minor channel (1/40 branching ratio) in this system and represents the only qualitative failure of our treatment.

The resulting peak for  $\text{O}^-$  production via the  $^2A_1$  state, at approximately 9.5 eV, is significantly larger than the experimental peak, just like our calculated  $\text{H}^-$  peak for this resonance [19]. We may have overestimated the magnitude of the entrance amplitude (we have calculated the partial width to be 10.30 meV [35]), or overestimated the survival probability. Both probabilities are directly affected by the lifetime of this metastable state as a function of nuclear geometry: a large entrance amplitude implies a small survival probability, and vice versa. However, the  $^2A_1$  state becomes a virtual



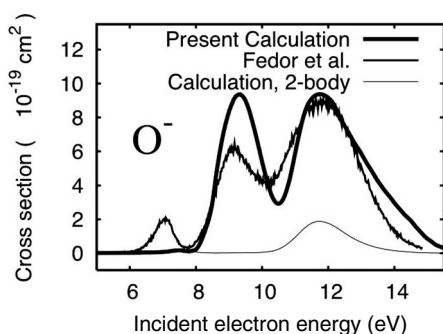


FIG. 3. Final results for  $O^-$  production in DEA to the water molecule, compared with the experimental results of Fedor *et al.* [10].

state at some geometries, and this fact has not been included in the current local complex potential model description. Virtual-state effects may lead to an enhanced autodetachment probability and a lower survival probability, i.e., may account for our overestimation of the physical cross section.

The three-body calculations on the  $^2B_2$  state resolve a significant discrepancy between our prior results for  $O^-$  pro-

duction [19] and that obtained by experiment; the magnitude of this peak is now reproduced accurately. Disagreement in the high-energy tail region may be due to the fact that the present calculation does not account for decay of the  $^2B_2$  state to the two-electron continuum.

Although it is not clear that our calculations within the local complex potential model include all the physical effects relevant to DEA of water, they appear to have reproduced the major features of experiment well, and demonstrate that three-body breakup is a major component of the observed  $O^-$  cross section.

D.J.H. acknowledges support at JILA, CU-Boulder, under DOE Grant No. W-31-109-ENG-38 and NSF Grant No. ITR 0427376. C.W.M. acknowledges support from the National Science Foundation under Grant No. PHY-0604628. D.J.H. thanks JILA's Center for Atomic, Molecular, and Optical Physics, funded by the NSF's Physics Frontier Center Program, for computer resources. Some of the work referenced in this paper was supported by DOE Contract No. DE-AC02-05CH11231 through the U.S. DOE Office of Basic Energy Sciences.

- [1] W. N. Lozier, *Phys. Rev.* **36**, 1417 (1930).  
 [2] I. S. Buchel'nikova, *Zh. Eksp. Teor. Fiz.* **35**, 1119 (1959).  
 [3] R. N. Compton and L. G. Christophorou, *Phys. Rev.* **154**, 110 (1967).  
 [4] C. E. Melton, *J. Chem. Phys.* **57**, 4218 (1972).  
 [5] L. Sanche and G. J. Schultz, *J. Chem. Phys.* **58**, 479 (1972).  
 [6] S. Trajmar and R. I. Hall, *J. Phys. B* **7**, L458 (1974).  
 [7] M. Jungen, J. Vogt, and V. Staemmler, *Chem. Phys.* **37**, 49 (1979).  
 [8] D. S. Belic, M. Landau, and R. I. Hall, *J. Phys. B* **14**, 175 (1981).  
 [9] M. G. Curtis and I. C. Walker, *J. Chem. Soc., Faraday Trans.* **88**, 2805 (1992).  
 [10] J. Fedor, P. Cicman, B. Coupier, S. Feil, M. Winkler, K. Gluch, J. Husarik, D. Jaksch, B. Farizon, and N. J. Mason, *J. Phys. B* **39**, 3935 (2006).  
 [11] C. R. Claydon, G. A. Segal, and H. S. Taylor, *J. Chem. Phys.* **54**, 3799 (1971).  
 [12] T. J. Gil, T. N. Rescigno, C. W. McCurdy, and B. H. Lengsfeld III, *Phys. Rev. A* **49**, 2642 (1994).  
 [13] J. D. Gorfinkel, L. A. Morgan, and J. Tennyson, *J. Phys. B* **35**, 543 (2002).  
 [14] D. J. Haxton, Z. Zhang, C. W. McCurdy, and T. N. Rescigno, *Phys. Rev. A* **69**, 062713 (2004).  
 [15] D. J. Haxton, Z. Zhang, H.-D. Meyer, T. N. Rescigno, and C. W. McCurdy, *Phys. Rev. A* **69**, 062714 (2004).  
 [16] D. J. Haxton, T. N. Rescigno, and C. W. McCurdy, *Phys. Rev. A* **72**, 022705 (2005).  
 [17] D. J. Haxton, C. W. McCurdy, and T. N. Rescigno, *Phys. Rev. A* **73**, 062724 (2006).  
 [18] D. J. Haxton, C. W. McCurdy, and T. N. Rescigno, *Phys. Rev. A* **75**, 012710 (2007).  
 [19] D. J. Haxton, T. N. Rescigno, and C. W. McCurdy, *Phys. Rev. A* **75**, 012711 (2007).  
 [20] D. T. Birtwistle and A. Herzenberg, *J. Phys. B* **4**, 53 (1971).  
 [21] L. Dube and A. Herzenberg, *Phys. Rev. A* **20**, 194 (1979).  
 [22] J. N. Bardsley and J. M. Wadehra, *J. Chem. Phys.* **78**, 7227 (1983).  
 [23] T. F. O'Malley, *Phys. Rev.* **150**, 14 (1966).  
 [24] T. F. O'Malley and H. S. Taylor, *Phys. Rev.* **176**, 207 (1968).  
 [25] C. W. McCurdy and J. L. Turner, *J. Chem. Phys.* **78**, 6773 (1983).  
 [26] H.-D. Meyer, U. Manthe, and L. S. Cederbaum, *Chem. Phys. Lett.* **165**, 73 (1990).  
 [27] U. Manthe, H.-D. Meyer, and L. S. Cederbaum, *J. Chem. Phys.* **97**, 3199 (1992).  
 [28] M. H. Beck, A. Jackle, G. A. Worth, and H.-D. Meyer, *Phys. Rep.* **324**, 1 (2000).  
 [29] G. A. Worth, M. H. Beck, A. Jackle, and H.-D. Meyer, Computer code MCTDH, Version 8.2 (University of Heidelberg, 2000); see <http://www.pci.uni-heidelberg.de/tc/usr/mctdh/>  
 [30] V. Kokoouline, C. H. Greene, and B. D. Esry, *Nature (London)* **412**, 891 (2001).  
 [31] L. M. Delves, *Nucl. Phys.* **9**, 391 (1959).  
 [32] L. M. Delves, *Nucl. Phys.* **20**, 275 (1960).  
 [33] D. J. Haxton, T. N. Rescigno, and C. W. McCurdy, in *Multi-dimensional Quantum Dynamics: MCTDH Theory and Applications*, edited by H.-D. Meyer, G. A. Worth, and F. Gatti (Wiley, Hoboken, NJ, in press).  
 [34] S. Feurbacher, T. Sommerfeld, and L. S. Cederbaum, *J. Chem. Phys.* **120**, 3201 (2004).  
 [35] S. Feurbacher and L. S. Cederbaum, *J. Chem. Phys.* **121**, 5 (2004).